Random-field critical and spin-flop behaviour of the anisotropic Heisenberg antiferromagnet $Fe_{0.85}Mg_{0.15}Br_2$ in axial magnetic fields

1994 J. Phys.: Condens. Matter 6 L75

(http://iopscience.iop.org/0953-8984/6/6/008)

J. Phys.: Condens. Matter 6 (1994) L75–L80. Printed in the UK

LETTER TO THE EDITOR

Random-field critical and spin-flop behaviour of the anisotropic Heisenberg antiferromagnet $Fe_{0.85}Mg_{0.15}Br_2$ in axial magnetic fields

M Karszewski†, J Kushauer†, Ch Binek†, W Kleemann† and D Bertrand‡

† Angewandte Physik, Universität Duisburg, D-47048 Duisburg, Germany

‡ Laboratoire de Physique des Solides associé au CNRS (URA 4), INSA, F-31077 Toulouse Cédex, France

Received 6 December 1993

Abstract. Faraday optical measurements on the dilute hexagonal antiferromagnet $Fe_{0.85}Mg_{0.15}Br_2$ in an external axial field reveal a spin-flop phase line ending at a multicritical point (T_m = 8.1 K, H_m = 1050 kA m^{-1}) and crossover from random-exchange to random-field Ising criticality with an exponent $\Phi = 1.40 \pm 0.04$ in the vicinity of T_N = 11.1 K. Cusp-like behaviour of the specific heat at T_N is discussed in view of recent Monte Carlo results.

The properties of disordered antiferromagnets (AFs) in an external magnetic field, H_a, have attracted considerable interest in recent years. In particular two ideas became a challenge to both theorists and experimentalists: (i) dilute uniaxial AFs in an axial field (DAFF) were proposed [1] and have been proven excellently [2] to exhibit the critical and the metastability properties of the ferromagnetic random-field Ising model (RFIM) [3]; (ii) solid solutions of AFs with competing anisotropies were predicted [4, 5] to show a rich variety of multicritical properties, parts of which were demonstrated by alloying AFs with Ising- and xy-type anisotropy, e.g. $FeCl_2$ with $CoCl_2$ [6] of $NiCl_2$ [7]. Interestingly, as predicted theoretically [1] these compounds also exhibit RFIM-type properties like DAFF systems when exposed to sub-multicritical fields [6, 7].

Important questions still remain open when considering both RFIM-type critical behaviour and multicritical properties of mixed uniaxial Heisenberg AF (UHAF) systems. On the one hand, the static scaling properties of the RFIM are still not completely settled. In particular, the value of the critical exponent of the specific heat, $\tilde{\alpha}$, is controversial. Whereas experiments [2] seem to favour $\tilde{\alpha} \sim 0$ for the RFIM in $d = 3$ dimensions, theoretical predictions range from $\tilde{\alpha} \sim 0.5$ according to scaling analysis [8] to $\tilde{\alpha} \sim -1$ as obtained by Monte Carlo (MC) simulations [9]. In this letter we present novel data on $Fe_{0.85}Mg_{0.15}Br_2$, which seem to corroborate cusp-like behaviour of the specific heat, and hence, $\tilde{\alpha} \sim -1$. Dynamic rounding due to precursor-type domain freezing [10] is, however, not excluded.

By chance, the same diluted system, $Fe_{0.85}Mg_{0.15}Br_2$, also widens the experimental view on the multicritical scenario depicted theoretically [5]. Very clearly a spin-flop (SF) phase is revealed ending at a multicritical point (MCP) at T_m = 8.1 K and H_m = 1050 kA m^{-1}. This is surprising, since the pure compound, $FeBr_2$, has been reported [11–13] to be metamagnetic below a tricritical point (TCP), T_m = 5.1 K and H_m = 2300 kA m^{-1}. In accordance with previous suggestions for $FeBr_2$ [14–16] a revision of the TCP conjecture in both pure and diluted $FeBr_2$ seems overdue. Very probably the MCPs observed in both systems correspond

0953-8984/94/060075+06$07.50

to critical endpoints (CEP). In $Fe_{0.85}Mg_{0.15}Br_2$ the CEP separates a low-temperature SF regime from a metamagnetic phase line despite the absence of any xy-type anisotropy, which is responsible for the SF phase, e.g. in $Fe_{0.5}Mg_{0.5}Cl_2$.

The experiments are carried out on Bridgman-grown samples of $Fe_{0.85}Mg_{0.15}Br_2$ as cleft to a thickness $t \sim 0.2$ mm parallel to planes perpendicular to the hexagonal c axis. Faraday rotation, θ, being proportional to the magnetization M [6,7], is measured with an accuracy $\Delta\theta < \pm 0.01°$ at a light wavelength $\lambda = 670$ mm of a laser diode in the temperature range $2.2 \leqslant T \leqslant 14$ K and in applied axial fields $H_a \leqslant 4000$ kA m^{-1} by using an apparatus described previously [6,7]. In isomagnetic measurements, H_a = constant, T is carefully stabilized to within $\delta T = 0.002$ K after each step-like change of $0.02 \leqslant |\Delta T| \leqslant 0.2$ K. Isotherms, θ versus H_a, are measured with field steps of $|\Delta H| \leqslant 5$ kA m^{-1}. Waiting times of about 30 s are allowed for equilibration at each new coordinate (H_a, T).

The H–T phase diagram is obtained from kinks and inflection points of isotherms and isomagnets, θ versus T, similarly to those found in previous work [6,7]. Figure 1(a) shows a typical isotherm recorded at $T = 2.21$ K as a function of H_a (curve a) and of the internal field $H = H_a - N\theta$ (curve b), respectively. The demagnetization factor N = 3.65 kA m^{-1} deg^{-1} is obtained empirically from correcting the finite peak of $\partial\theta/\partial H_a$ at $H_{a,c1}$ = 1610 kA m^{-1} (curve a′) to become divergent with virtually vanishing width, $\delta H \simeq 0$, at H_{c1} = 1500 kA m^{-1} (curve b′). This procedure follows previous analysis of θ versus H_a curves [6], where a SF phase is reached via a first-order AF–SF transition. As a function of H_a this transition is smeared over a finite field range, $\delta H_a \sim 250$ kA m^{-1} in the present case of $Fe_{0.85}Mg_{0.15}Br_2$. It corresponds to a mixed AF–SF phase. Above H_{c1}, linear increase of θ versus H characterizes the SF phase. At $H_{a,c2} \sim 2400$ kA m^{-1} and $H_{c2} \sim$ 1700 kA m^{-1}, respectively, magnetic saturation, $\theta \sim 270°$, in the paramagnetic (PM) phase is smoothly reached. The situation resembles that of $Fe_{0.73}Co_{0.27}Cl_2$ [6], where random anisotropy (RA) effects [17] are assumed to cause the observed smearing. In fact, owing to off-diagonal spin–spin interaction being active in the SF phase [6] RA should play a role also in a dilute system like $Fe_{0.85}Mg_{0.15}Br_2$.

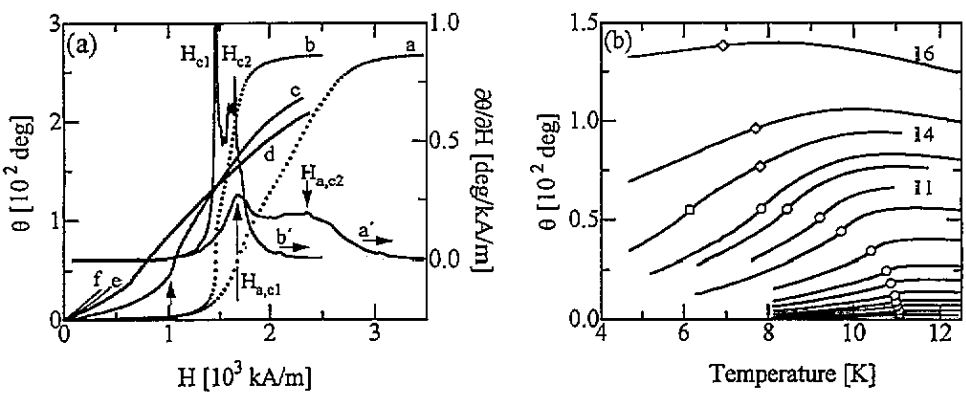

Figure 1. (a) Faraday rotation θ versus the applied (a) and internal field (b–f), at $T = 2.21$ (a), (b), 8.14 (c), 9.95 (d), 10.51 (e) and 11.31 K (f). Derivative curves $\partial\theta/\partial H$ versus the applied (a′) and internal field (b′) are shown for $T = 2.21$ K together with the phase transition fields H_{c1}, H_{c2} and $H_{a,c2}$ (arrow). The arrow on curve c indicates the first-order AF–PM transition. (b) θ versus T measured at applied fields H_a (from bottom to top) = 33 (1), 49 (2), 72 (3), 115 (4)m, 154 (5), 220 (6), 316 (7), 438 (8), 641 (9), 898 (10), 1044 (11), 1210 (12), 1290 (13), 1450 (14), 1610 (15) and 2020 kA m^{-1} (16). Phase transition temperatures are marked by circles, diamonds and squares (see the text).

With increasing temperature the linear part of the θ versus H curve is shrinking. It disappears at $T > 8.1$ K (figure 1(a), curve c), whereas the divergence of $\partial\theta/\partial H$ still remains visible. The corresponding sharp kink in θ versus H survives up to $T \sim 9$ K (arrow in curve c) and seems to indicate a first-order AF–PM phase line.

Typical isomagnets recorded in fields $33 \leqslant H_a \leqslant 2020$ kA m^{-1} between 4.5 and 13 K are shown in figure 1(b). Similarly to what was argued for $Fe_{1-x}M_xCl_2$ (M = Co [6] and Ni [7]) points of inflection characterize AF–PM transitions (circles in figure 1(b)), whereas kinks (diamonds) are typical of SF–PM transitions, both of them being second order. Below the kink points the SF phase exhibits a linear θ versus T dependence (curves 14–16). Another kink point at low T (the square on curve 14) indicates the first-order AF–SF transition.

Figure 2 shows the H_a–T (a) and the H–T (b) phase diagrams thus constructed. The approximate width of the mixed AF–SF phase around $H_{a,cl}$ is indicated by error bars. The MCP, where AF, SF and PM phases coexist, is determined as $T_m = (8.1 \pm 0.1)$ K, $H_{a,m} = 1300 \pm 50$ kA m^{-1} and $H_m = 1050 \pm 50$ kA m^{-1}, respectively. Lacking the typical umbilicus shape, the MCP is very probably not bicritical, but is rather a CEP. Similarly to what was argued in the case of $Fe_{1-x}Ni_xCl_2$ [7] a CEP is expected to occur in spin $S = 1$ systems for intermediate anisotropy and sufficiently large ferromagnetic (FM) next-nearest-neighbour (NNN) exchange interaction [5]. Note that for the layered AF $FeBr_2$ the NNN exchange refers to the effective FM in-plane interaction, whereas the interplanar AF bonds are denoted as NN [7].

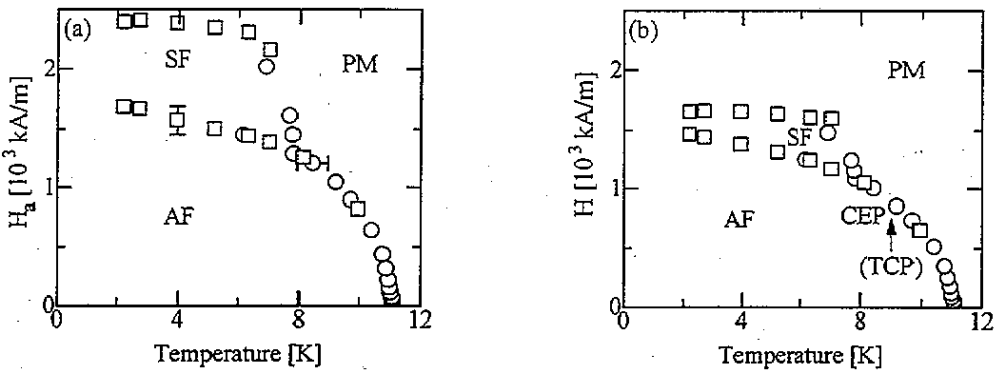

Figure 2. The phase diagrams H_a versus T (a) and H versus T (b) of $Fe_{0.85}Mg_{0.15}Br_2$ obtained from isothermal (squares) and isomagnetic (circles) FR data (figure 1(a) and (b)). The paramagnetic (PM), antiferromagnetic (AF) and spin-flop (SF) ranges, the critical endpoint (CEP) and the tentative tricritical point (TCP) are indicated. The approximate width of the mixed AF–SF phase is indicated by an error bar in figure 2(a).

The first-order AF–PM phase boundary extends between the CEP and a tricritical point (TCP), $T_t \sim 9$ K and $H_t \sim 900$ kA m^{-1}. Within the framework of the mean-field theory [5] a phase diagram close to that shown in figure 2(b) emerges for $Fe_{0.5}Ni_{0.5}Cl_2$ [7] with the exchange and anisotropy parameters $e_1 = 10.56$ and $d = 0.9$, respectively. These numbers refer to the FM NNN exchange and to the single-ion anisotropy normalized to the AF NN exchange constant. For $FeBr_2$ we find $e_1 = 2.51$ and $d = 1.45$ when using Vettier's energy parameters [18] and taking into account 20 NN bonds in the D^3_{3d} space group of $FeBr_2$ [19]. Within the general topology of multicritical points and surfaces in the T–e_1–d parameter space of UHAF systems [5], the two above sets of parameters are expected to

yield qualitatively similar phase diagrams. The $Fe_{0.85}Mg_{0.15}Br_2$ system considered here is described by $e_1 = 2.51$ and $d = 1.67$, taking into account that all exchange parameters decrease by 15% due to the dilution, whereas the single-ion anisotropy remains unchanged. The enhancement of d is expected [5] merely to widen the metamagnetic gap between T_m and T_t compared with the (hitherto undetected) one of $FeBr_2$. Clearly, explicit calculations along the lines of the mean-field theory within the virtual-crystal [5] or probabilistic molecular-field approximation [20] are necessary for a better understanding of the observed phase diagram. In parallel, however, clearer knowledge of the $FeBr_2$ phase diagram is urgently needed.

In the low-H range, $H \ll H_t$, H_m, $Fe_{0.85}Mg_{0.15}Br_2$ exhibits crossover from the random-exchange Ising model (REIM) to RFIM critical behaviour. This is verified by the double-logarithmic plot of $T_N - T_c(H) - bH^2$ versus H in figure 3(a). $T_c(H)$ refers to data shown in figure 2(b), whereas the Néel temperature $T_N = 11.11$ K and the mean-field correction $b = 8 \times 10^{-8}$ K kA^{-2} m^{-2} are obtained from the straight line in figure 3(a), best fitted to the data for $H < 900$ kA m^{-1}. Its slope equals $2/\Phi$ [2], where $\Phi = 1.43 \pm 0.06$ is the REIM–RFIM crossover exponent. This value agrees with previous results on other DAFF systems [2], including $Fe_{0.7}Mg_{0.3}Cl_2$ [21] and $Fe_{0.73}Co_{0.27}Cl_2$ [6].

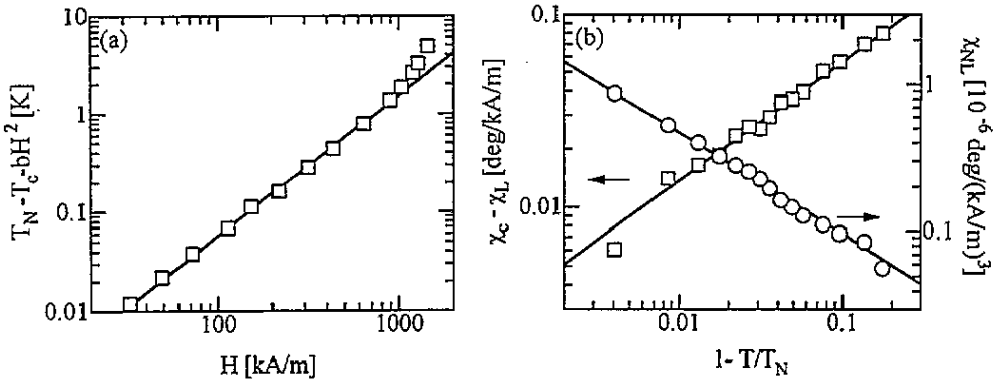

Figure 3. (a) A log–log plot of $T_N - T_c(H) - bH^2$ versus H (squares) and a straight line, best fitted for $33 \leqslant H \leqslant 900$ kA m^{-1} with $T_N = 11.11$ K and $b = 8 \times 10^{-8}$ K kA^{-2} m^{-2}. (b) Log–log plots of $\chi_c - \chi_L$ (squares) and χ_{NL} (circles) versus reduced temperature $1 - T/T_N$, where $\chi_c = \chi_L(T_N) = 0.14°$ kA^{-1} m^{-1} and $T_N = 11.06$ K.

The same value, within errors is obtained from the following FR study of the linear and the non-linear susceptibilities χ_L and χ_{NL}, in the limit $H = 0$. According to scaling theory [22] they are expected to diverge at T_N with exponents $2\beta' = 2-\alpha-\Phi$ and $\gamma' = 2-\alpha-2\Phi$, respectively, where α is the REIM critical exponent of the specific heat. Analysing near-critical isotherms in the vicinity of T_N (e.g. figure 1(a), curves e, f) by use of the expansion $\chi = \chi_L H + \chi_{NL} H^3/3 + O(H^5)$ [21] we find $2\beta' = 0.66 \pm 0.02$ and $\gamma' = -0.72 \pm 0.02$ from log–log plots of $\chi_c - \chi_L$ and χ_{NL} versus $1 - T/T_N$ (figure 3(b)), where $\chi_c = \chi_L(T_N)$. We thus obtain $\Phi = 1.38 \pm 0.04$ and $\alpha = -0.04 \pm 0.06$ in agreement with expected values and those obtained by the same method for $Fe_{0.7}Mg_{0.3}Cl_2$ [21]. Note that these data refer to a sample with $T_N = 11.06$ K, the Mg^{2+} concentration of which is slightly larger than that used for the data in figure 3(a).

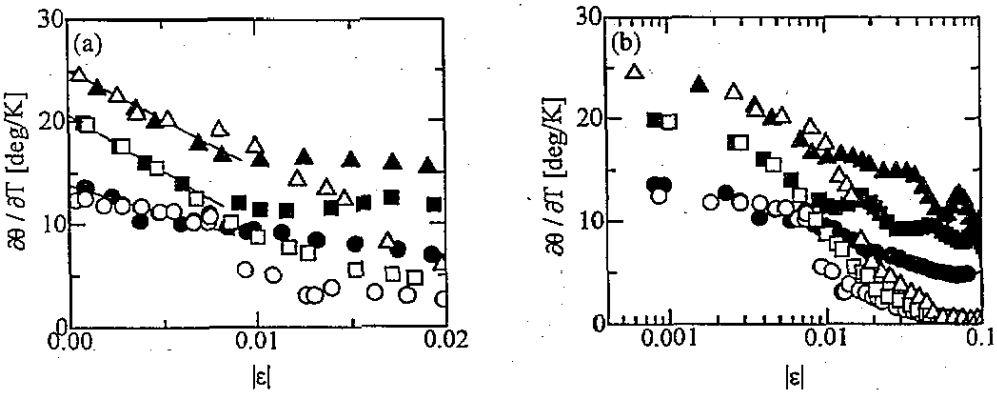

Figure 4. Linear (a) and logarithmic (b) plots of $\partial\theta/\partial T$ versus $|\epsilon| = |T - T_c(H_a)|/T_N$ with straight lines as guides to the eye (a) for H_a = 200 (circles), 320 (squares) and 440 kA m^{-1} (triangles). Open (full) symbols refer to $T > T_c$ ($T < T_c$).

Static critical behaviour in the low-H RFIM range emerges from $(\partial\theta/\partial T)_H$ versus T. It is expected [23] to scale as $H^y|\epsilon|^{-\tilde{\alpha}}$, where $y = 2(1 + \tilde{\alpha} - \alpha - \Phi/2)/\Phi$ and $\tilde{\alpha}$ is the RFIM exponent of the specific heat. Data taken from θ versus T curves (see, e.g., figure 1(b)) for H_a = 200, 320 and 440 kA m^{-1} are plotted in figure 4 versus $|\epsilon| = |T - T_c(H_a)|/T_N$, (a), and $\log_{10}|\epsilon|$, (b), respectively. As observed for other DAFF systems [2, 6, 22] the branches for $\epsilon > 0$ and $\epsilon < 0$ coincide close to $T_c(H_a)$, $|\epsilon| < 10^{-2}$. At a closer look it is obvious that the linear functions (a) are much better approximated by straight lines that the logarithmic ones (b). The latter are bent in a convex manner as $|\epsilon| \to 0$, hence indicating cusp-like behaviour rather than a logarithmic singularity with $\tilde{\alpha} = 0$. It should be noticed that similar convexities were also revealed by $(\partial\theta/\partial T)_H$ versus T data on $Fe_{0.7}Mg_{0.3}Cl_2$ [21]. The linear functions $(\partial\theta/\partial T)_H = a - b|\epsilon|$, with constants a and b, seem to favour $\tilde{\alpha} \sim -1$, in agreement with the simulation result, $\tilde{\alpha} = -1.0 \pm 0.3$ [9]. This implies, however, serious contradictions to conventional scaling predictions. These yield, for example, $y \sim -0.9$ and an order parameter exponent $\tilde{\beta} = (2 - \tilde{\alpha} - \tilde{\gamma})/2 \sim 0.6$ with $\tilde{\gamma} = 1.75$ [2], both of which disagree with present experimental evidence [2]. Very probably our novel data do not give a conclusive solution to these problems. Similarly to what was argued previously [10], despite waiting times $\tau > 10$ s, dynamic rounding might lie at the origin of the observed cusp-like behaviour.

Another important consequence of the extreme critical slowing down is the formation of a metastable domain state when field cooling DAFF systems to below $T_c(H)$ [10]. Very typically, they are accompanied by excess magnetization ΔM, in comparison with that of the long-range ordered ground state. Similarly to what was described for $Fe_{0.73}Co_{0.27}Cl_2$ [6], we observe a strong smearing of the SF–AF transition when crossing the phase line of $Fe_{0.85}Mg_{0.15}Br_2$ within the temperature range $2.2 \leqslant T \leqslant 7.1$ K (figure 2) by decreasing the field. Just below H_{c1} (figure 1(a)) we find the maximum excess FR, $\Delta\theta \propto 1/T$. This relation is expected to hold if ΔM is primarily stored in the walls of the AF domains with size $R \propto T$ [10].

In conclusion, we have shown that the diluted UHAF system $Fe_{0.85}Mg_{0.15}Br_2$ reveals conventional REIM–RFIM crossover behaviour, whereas the question on the asymptotic value of the critical exponent $\tilde{\alpha}$ still seems to be open. Unexpectedly, it exhibits novel multicritical behaviour. Evidence for a low-T SF phase has been given, which casts doubts on the

metamagnetism hitherto reported for the pure compound $FeBr_2$.

This work was supported by Deutsche Forschungsgemeinschaft through 'Sonderforschungsbereich 166'.

References

[1] Fishman S and Aharony A 1979 *J. Phys. C: Solid State Phys.* **12** L729
[2] For recent reviews, see
Belanger D P 1988 *Phase Transitions* **11** 53
Jaccarino V and King A R 1990 *Physica* A **163** 29
[3] Imry Y and Ma S K 1975 *Phys. Rev. Lett.* **35** 1399
[4] Kincaid J M and Cohen E G D 1975 *Phys. Rep.* **22** 57
[5] Vilfan I and Galam S 1986 *Phys. Rev.* B **34** 6428
[6] Nitsche W and Kleemann W 1988 *Phys. Rev.* B **37** 7680
[7] Igel B, Kleemann W and Vilfan I 1990 *J. Phys.: Condens. Matter* **2** 4495
Cleve E and Kleemann W 1991 *Phase Transitions* **37** 73
[8] For a review, see
Nattermann T and Villain J 1988 *Phase Transitions* **11** 5
[9] Rieger H and Young A P 1993 *J. Phys. A: Math. Gen.* **26** 5279
[10] For a review, see
Kleemann W 1993 *Int. J. Mod. Phys.* B **7** 2469
[11] Wilkinson M K, Cable J W, Wollan E O and Koehler W C 1959 *Phys. Rev.* **113** 497
[12] Jacobs I S and Lawrence P E 1967 *Phys. Rev.* **164** 866
[13] Fert A R, Carrara P, Lanusse M C, Mischler G and Redoulès J P 1973 *J. Phys. Chem. Solids* **34** 223
[14] Stryjewski E and Giordano N 1977 *Adv. Phys.* **26** 487
[15] Onyszkiewicz Z 1980 *Physica* A **103** 226; 274
[16] Wood T E, Muirhead A and Day P 1978 *J. Phys. C: Solid State Phys.* **11** 1619
[17] Oku M and Igarashi H 1983 *Prog. Theor. Phys.* **70** 1493
[18] Vettier C 1975 *Thèse d'Etat* Grenoble
[19] Hernandez L, Diep H T and Bertrand D 1993 *Europhys. Lett.* **21** 711
[20] Seier J, Usadel K D and Moschel A 1991 *J. Phys.: Condens. Matter* **3** 9733
[21] Leitão U A and Kleemann W 1987 *Phys. Rev.* B **35** 8696; 1988 *Europhys. Lett.* **5** 529
[22] Aharony A 1986 *Europhys. Lett.* **1** 617
[23] Kleemann W, King A and Jaccarino V 1986 *Phys. Rev.* B **34** 479